Published in final edited form as:

Cell Rep. 2018 May 08; 23(6): 1716–1727. doi:10.1016/j.celrep.2018.03.130.

A Glutamate Homeostat Controls the Presynaptic Inhibition of Neurotransmitter Release

Xiling Li[1,2,4], **Pragya Goel**[1,3,4], **Joyce Wondolowski**[1], **Jeremy Paluch**[1], and **Dion Dickman**[1,5,*]

[1]Department of Neurobiology, University of Southern California, Los Angeles, CA

[2]USC Neuroscience Graduate Program, University of Southern California, Los Angeles, CA

[3]USC Graduate Program in Molecular and Computational Biology, University of Southern California, Los Angeles, CA

Summary

We have interrogated the synaptic dialog that enables the bi-directional, homeostatic control of pre-synaptic efficacy at the glutamatergic *Drosophila* neuromuscular junction (NMJ). We find that homeo-static depression and potentiation use disparate genetic, induction, and expression mechanisms. Specifically, homeostatic potentiation is achieved through reduced CaMKII activity postsynaptically and increased abundance of active zone material presynaptically at one of the two neuronal subtypes innervating the NMJ, while homeostatic depression occurs without alterations in CaMKII activity and is expressed at both neuronal subtypes. Furthermore, homeostatic depression is only induced through excess presynaptic glutamate release and operates with disregard to the postsynaptic response. We propose that two independent homeostats modulate presynaptic efficacy at the *Drosophila* NMJ: one is an intercellular signaling system that potentiates synaptic strength following diminished postsynaptic excitability, while the other adaptively modulates presynaptic glutamate release through an autocrine mechanism without feedback from the postsynaptic compartment.

Graphical abstract

*Correspondence: dickman@usc.edu.
[4]These authors contributed equally
[5]Lead Contact

Supplemental Information: Supplemental Information includes Supplemental Experimental Procedures, five figures, and one table and can be found with this article online at https://doi.org/10.1016/j.celrep.2018.03.130.

Author Contributions: X.L. and P.G. obtained all experimental data. J.W. and J.P. contributed electrophysiological data at elevated temperatures. X.L., P.G., and D.D. analyzed and interpreted all data. The manuscript was written by D.D. with comments from P.G. and X.L.

Declaration of Interests: The authors declare no competing interests.

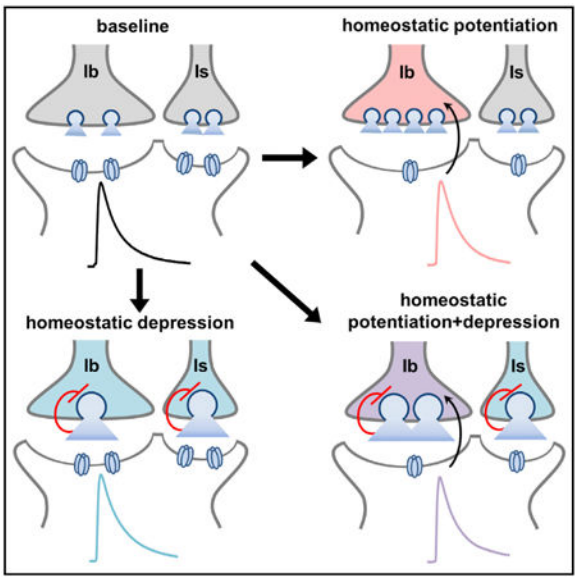

Homeostatic mechanisms stabilize synaptic strength, but the signaling systems remain enigmatic. Li et al. suggest the existence of a homeostat operating at the *Drosophila* neuromuscular junction that responds to excess glutamate through an autocrine mechanism to adaptively inhibit presynaptic neurotransmitter release. This system parallels forms of plasticity at central synapses.

Introduction

Synapses have the remarkable ability to adaptively modulate synaptic strength when confronted with diverse challenges that destabilize neurotransmission, yet the mechanisms controlling the integration of these responses remain enigmatic. Homeostatic mechanisms operate to stabilize synaptic activity in nervous systems of varied organisms ranging from invertebrates to humans (Pozo and Goda, 2010). In these physiological systems, destabilizing perturbations to neurotransmission are offset by compensatory adaptations to postsynaptic neurotransmitter receptors (synaptic scaling) and/or presynaptic efficacy that maintains normal levels of functionality (Davis and Müller, 2015; Turrigiano, 2012). This phenomenon, termed homeostatic synaptic plasticity, is thought to interface with Hebbian plasticity mechanisms to ensure stable yet flexible ranges in synaptic strength (Turrigiano, 2017). While adaptive responses to individual destabilizing perturbations have been characterized in significant detail, less is known about how homeostatic signaling systems integrate reactions to concurrent challenges, particularly when these are in conflict.

The *Drosophila* neuromuscular junction (NMJ) is a powerful model system to study the bi-directional, homeostatic control of synaptic strength. At this glutamatergic synapse, acute pharmacological and chronic genetic manipulations that reduce postsynaptic glutamate receptor (GluR) function activate a retrograde, *trans*-synaptic signaling system that triggers a compensatory increase in presynaptic glutamate release, restoring baseline levels of synaptic strength (Frank, 2014). Because the expression of this form of plasticity requires a presynaptic increase in neurotransmitter release, this process is referred to as presynaptic homeostatic potentiation (PHP). Multiple lines of evidence have established that the

homeostat that governs PHP is exquisitely sensitive to diminished postsynaptic excitability and operates through a retrograde enhancement of pre-synaptic efficacy, stabilizing overall synaptic strength (Frank et al., 2006; Petersen et al., 1997). Parallel phenomena have been observed at cholinergic NMJs in rodents and humans (Cull-Candy et al., 1980), suggesting this is a fundamental and conserved form of synaptic plasticity that does not depend on the neurotransmitter system.

In contrast to PHP, far less is known about the homeostat that governs an inverse process at the *Drosophila* NMJ, referred to as presynaptic homeostatic depression (PHD). The first evidence for PHD, although not appreciated as such, was discovered while characterizing mutations in synaptic vesicle endocytosis genes, in which increased synaptic vesicle size was found to result from defects in vesicle re-formation mechanisms (Chen et al., 2014; Dickman et al., 2005; Marie et al., 2004; Verstreken et al., 2002). Independently, evidence for PHD was found using a separate manipulation that also increased synaptic vesicle size through overexpression of the vesicular glutamate transporter (*vGlut*; vGlut-OE) (Daniels et al., 2004). Both defective endocytosis and vGlut-OE result in enlargement of individual synaptic vesicles, leading to excess glutamate emitted from each synaptic vesicle and enhanced postsynaptic responsiveness (quantal size). However, normal levels of synaptic strength (excitatory postsynaptic potential [EPSP] amplitude) were observed due to a homeostatic reduction in the number of synaptic vesicles released (quantal content). When the phenomenon of PHD was initially defined, one hypothesis put forward was that PHD may be induced as an adaptive response to excess glutamate (Daniels et al., 2004). More recently, PHD has been considered a mechanism that stabilizes neurotransmission in the same way that PHP operates (Gaviño et al., 2015), implying that PHD is calibrated as a homeostat that responds to overall synaptic strength. Despite these studies, the nature of the homeostat that controls PHD, as well as the genes and mechanisms involved, remains much less understood relative to PHP. It is not even clear whether *trans*-synaptic communication is required to induce, express, or modulate PHD.

We have characterized the adaptations to synaptic physiology, growth, structure, and plasticity when PHP and PHD are induced and expressed alone and in conjunction at an individual synapse. Several lines of evidence demonstrate that PHP and PHD are independent processes that use distinct mechanisms to modulate presynaptic efficacy in opposing directions and operate at separate neuronal subtypes. However, PHP and PHD are not simply independent signaling systems that each tune presynaptic efficacy to maintain stable levels of synaptic strength. Rather, our data indicate that PHP is indeed a homeostat dedicated to maintaining synaptic strength, induced through retrograde signaling in the postsynaptic compartment. In contrast, PHD operates with indifference to the state of the postsynaptic cell and is oblivious to overall synaptic strength, instead functioning cell autonomously in the presynaptic neuron as a negative feedback system to homeostatically modulate glutamate release.

Results

Bi-directional, Homeostatic Control of Presynaptic Efficacy at the *Drosophila* NMJ

Homeostatic regulation of presynaptic glutamate release can be induced and expressed at the *Drosophila* NMJ. To characterize the mechanisms underlying PHD alone and when PHP and PHD are combined at an individual synapse, we used four distinct conditions (schematized in Figure 1A). Genetic mutations in the postsynaptic GluR subunit *GluRIIA* were used to assess the chronic expression of PHP. In this mutant, reduced miniature excitatory postsynaptic potential (mEPSP) amplitude, but normal EPSP amplitude, is observed due to a homeostatic increase in presynaptic glutamate release (quantal content) (Figures 1A–1E). To induce PHD, we overexpressed *vGlut* in motor neurons (vGlut-OE). This increases mEPSP amplitude, but synaptic strength is similar to wild-type levels because of a homeostatic reduction in quantal content (Figures 1A–1E). Thus, in both PHP and PHD, quantal content is inversely adjusted relative to quantal size, maintaining constant levels of synaptic strength.

We next probed how a synapse adapts to a combination of genetic manipulations that individually induce PHP or PHD expression. When we combined *GluRIIA* and vGlut-OE (*GluRIIA*+vGlut-OE), quantal size was intermediate to either manipulation alone (Figure 1C), consistent with reduced postsynaptic GluR expression but increased glutamate released per vesicle. Nonetheless, EPSP amplitude and quantal content are maintained at levels similar to control values (Figures 1A, 1D and 1E). We confirmed the expected *GluRIIA* and *vGlut* expression in all four genotypes (Figure S1). Finally, we observed robust scaling of quantal content as a function of mEPSP amplitude in all genotypes, including *GluRIIA* +vGlut-OE (Figure 1F), consistent with sensitivity of the homeostat to presynaptic glutamate release and/or postsynaptic responsiveness. Thus, presynaptic glutamate release is under exquisite, bi-directional, homeostatic modulation and can be induced, expressed, and balanced at an individual synapse, maintaining stable levels of synaptic strength over chronic timescales.

Conventional Mechanisms Drive the Acute Expression of PHP in a Chronically Depressed Synapse

PHP can be rapidly induced and expressed using an acute pharmacological method to block postsynaptic GluRs with the antagonist philanthotoxin-433 (PhTx) (Frank et al., 2006). A previous study reported the important demonstration that PHP can be acutely expressed at vGlut-OE NMJs (Gaviño et al., 2015), as we have shown over chronic timescales (*GluRIIA* +vGlut-OE). We first confirmed this result by applying PhTx to vGlut-OE NMJs, which resulted in the expected ~50% reduction in mEPSP amplitude and a robust increase in quantal content, maintaining the homeostatic control of EPSP amplitude (Figures 2A–2C). Thus, presynaptic neurotransmitter release can be acutely potentiated despite chronic depression induced by vGlut-OE, balancing overall synaptic strength.

To assess whether conserved genetic mechanisms underlie PHP and PHD, we asked whether the schizophrenia susceptibility gene *dysbindin (dysb),* necessary in motor neurons for both acute and chronic forms of PHP expression (Dickman and Davis, 2009), is required for PHD expression. We observed no difference in quantal content when vGlut-OE was combined

with *dysbindin* mutations (*dysb*+vGlut-OE) (Figures 2D–2F), suggesting that *dysbindin* plays no role in PHD induction or expression, consistent with separate genetic mechanisms driving PHP and PHD (Gaviño et al., 2015; Kiragasi et al., 2017). We also probed whether conventional PHP expression mechanisms remain utilized when PHP is induced at a homeostatically depressed synapse. We applied PhTx to *dysb*+vGlut-OE synapses and observed a failure to homeostatically potentiate quantal content (Figures 2D–2F) while PHD was normally expressed. Therefore, conventional genetic mechanisms are required for the acute induction of PHP at a synapse expressing PHD, while PHP and PHD use separate genetic expression mechanisms that are effectively superimposed when balanced at an individual synapse.

Ca^{2+} Cooperativity, Release Probability, and Vesicle Pools Are Balanced in *GluRIIA*+vGlut-OE

PHP and PHD use shared but inverse changes in Ca^{2+} influx at presynaptic terminals (Gaviño et al., 2015; Müller and Davis, 2012), but only PHP appears to involve modulation of the readily releasable synaptic vesicle pool (RRP) when examined individually (Gaviño et al., 2015; Müller et al., 2012). However, it is unclear how these expression mechanisms are integrated when combined at an individual synapse. We first measured the apparent Ca^{2+} cooperativity of neurotransmission by examining quantal content over a range of external Ca^{2+} concentrations. We observed no significant difference in the apparent Ca^{2+} cooperativity in *GluRIIA*+vGlut-OE (Figure 3A), which showed a similar slope compared to wild-type, *GluRIIA*, and vGlut-OE. Furthermore, we found significant differences in excitatory postsynaptic current (EPSC) amplitudes at elevated Ca^{2+} concentrations across all genotypes (Figure 3B). Altogether, this demonstrates presynaptic glutamate release is properly tuned across a range of Ca^{2+} conditions following individual or simultaneous expression of PHP and PHD at a single synapse.

We next performed a series of experiments to probe release probability (P_r) in *GluRIIA* mutants, vGlut-OE, and *GluRIIA*+ vGlut-OE. Failure analysis assesses presynaptic function independently of mEPSP amplitude, which has been used to show that *GluRIIA* mutants exhibit fewer failures (Petersen et al., 1997), whereas vGlut-OE displays increased failure rates (Daniels et al., 2004). We observed the expected decrease in failure rate in *GluRIIA* mutants (consistent with increased P_r) and increase in failures in vGlut-OE relative to wild-type (consistent with reduced P_r) (Figure 3C). Failure rate in *GluRIIA*+vGlut-OE was intermediate and not significantly different from that of wild-type, consistent with balancing of PHP and PHD modulations (Figure 3C). In addition, paired-pulse ratios have been used to gauge P_r, in which depression or facilitation is observed in the second stimulus evoked shortly after an initial stimulus. At physiological Ca^{2+} conditions (1.5 mM), paired-pulse depression (PPD) is observed at the *Drosophila* NMJ (Böhme et al., 2016). We found enhanced PPD in *GluRIIA* mutants, reduced PPD in vGlut-OE, and no significant difference in *GluRIIA*+vGlut-OE compared to wild-type (Figures 3D and 3E). Similarly, no change in paired-pulse facilitation (PPF) is observed in reduced extracellular Ca^{2+} (0.3 mM) in *GluRIIA*+vGlut-OE, while reduced and enhanced PPF is observed in *GluRIIA* and vGlut-OE, respectively (Figures 3F and 3G). Hence, the results of failure analysis, PPD, and PPF are consistent with PHP exhibiting increased P_r, vGlut-OE showing reduced P_r, and overall

P_r being similar to wild-type when these opposing modulations are simultaneously expressed.

An increase in the RRP is induced at synapses following acute and chronic expression of PHP (Kiragasi et al., 2017; Müller et al., 2012; Weyhersmüller et al., 2011), but no changes in this vesicle pool are observed at synapses expressing PHD (Gaviño et al., 2015). We therefore measured the RRP in *GluRIIA*+vGlut-OE, a situation in which we would predict an increase in the RRP as part of PHP expression, and no overall change contributed by PHD. We performed two-electrode voltage-clamp (TEVC) recordings in 3 mM external Ca^{2+}, stimulating at 60 Hz and measuring the cumulative EPSC (Figures 3H–3K). We observed the expected increase in the RRP in *GluRIIA* mutants, no change in vGlut-OE, and an increase in *GluRIIA*+vGlut-OE (Figure 3I). Thus, one key expression mechanism underlying PHP, an increase in the RRP, can be fully induced at synapses also expressing PHD, demonstrating that PHD induction does not occlude the mechanisms necessary for PHP expression.

Finally, vGlut-OE enlarges synaptic vesicle size (Daniels et al., 2004), which may have secondary impacts on vesicle biogenesis, membrane trafficking, and/or mobility that could alter synaptic physiology. We therefore measured the entire releasable synaptic vesicle pool size in vGlut-OE using a temperature-sensitive allele of *shibire (shi),* the fly homolog of the endocytic gene *dynamin* (Kidokoro et al., 2004). In this mutation, all forms of synaptic vesicle endocytosis are blocked at the restrictive temperature (32°C) due to a failure of vesicle scission from the membrane. In *shi* mutant synapses, release ceased after ~350 s, demonstrating that all releasable synaptic vesicles had been depleted (Figure S2A). We found that the total releasable vesicle pool was equivalent in *shi* to that in *shi;GluRIIA, shi*;vGlut-OE, and *shi*;*GluRIIA*+vGlut-OE NMJs (~88,000 total quanta) (Figure S2B). Thus, the total releasable synaptic vesicle pool is unchanged despite the enlargement of individual vesicles due to vGlut-OE.

The Active Zone Scaffold BRP and Ca^{2+} Channel Cac Are Enhanced Specifically at Type Ib Boutons in *GluRIIA* Mutants

It is unknown whether an anatomical change contributes to the stabilization of synaptic strength in vGlut-OE alone or in *GluRIIA*+vGlut-OE. Synaptic growth may be affected by enlarged vesicle size, perhaps altering the balance of constitutive versus regulated membrane trafficking during development (Kikuma et al., 2017). Most muscles in *Drosophila* receive input from two motor neurons exhibiting morphologically distinct terminals, type Is (type I small) and type Ib (type I big) (Atwood et al., 1993), but synaptic growth at these terminals has not been defined in *GluRIIA* mutants or vGlut-OE. We found a small reduction in the number of type Ib boutons in *GluRIIA* mutants, which was also observed in vGlut-OE and *GluRIIA*+vGlut-OE (Figures S3A–S3D). Surprisingly, we observed an increase in type Is boutons in both vGlut-OE and *GluRIIA*+vGlut-OE, with no change in *GluRIIA* mutants (Figures S3A–S3D), leading to no difference in total bouton number per NMJ (Figure S3E). The reason for enhanced synaptic growth at type Is boutons in vGlut-OE is unclear but may be related to the enlarged synaptic vesicles and possibly enhanced membrane conferred at this high *Pr* neuronal subtype. We also observed no significant difference in the density of

active zones labeled by the active zone scaffold bruchpilot (BRP) in either type Ib or type Is terminals (Figures S3B–S3F) or in active zone-GluR apposition (Table S1). Thus, PHP and PHD expression have distinct influences on synaptic growth at the type Ib and type Is motor neuron subtypes.

We next assessed active zone structure at synaptic terminals of *GluRIIA* mutants. The intensity of BRP does not change at either type Ib or type Is boutons in vGlut-OE (Gaviño et al., 2015). However, while an enhancement in BRP intensity occurs in *GluRIIA* mutants and following PhTx application (Goel et al., 2017; Weyhersmüller et al., 2011), this remodeling has not been defined at type Ib vs type Is boutons. We therefore imaged individual BRP puncta and found a significant increase in both the mean and sum puncta intensity in *GluRIIA* mutants at terminals of type Ib boutons (Figures 4A–4C), while no significant change was seen at type Is (Figures 4F–4H), consistent with PHP signaling and BRP remodeling happening specifically at type Ib boutons. Next, we assessed intensity of the Ca^{2+} channel Cac in *GluRIIA* mutants using overexpression of a GFP-tagged transgenic allele of this channel (Cac-GFP-OE). A reduction in Cac-GFP-OE abundance was reported at both type Is and type Ib terminals in vGlut-OE (Gaviño et al., 2015), but has not been assessed following chronic PHP expression. We found a corresponding increase in Cac-GFP intensity (both mean and sum) at active zones specifically at type Ib terminals, with no change at type Is (Figures 4A–4J). Consistent with this result, endogenously tagged Cac-GFP channels are also enhanced at type Ib terminals following acute PhTx application (Gratz et al., 2018). Thus, both the active zone scaffold BRP and Ca^{2+} channel Cac are remodeled and augmented specifically at type Ib terminals in *GluRIIA* mutants, consistent with PHP expression restricted to type Ib inputs found through functional studies (Newman et al., 2017). These adaptations presumably contribute to the increased Ca^{2+} influx (Müller and Davis, 2012) and P_r that drive PHP expression.

Ca^{2+} Imaging Reveals PHD Is Functionally Expressed at Both Type Is and Type Ib Inputs

PHD expression at terminals of neuronal type Ib versus type Is neuronal subtypes has not been functionally defined. A Ca^{2+} indicator was developed and used to show that PHP is expressed exclusively at type Ib boutons at the *Drosophila* NMJ (Newman et al., 2017). This indicator, SynapGCaMP6f, targets GCaMP6f to the postsynaptic density and enables robust quantal imaging at type Ib and Is terminals. Active zones of type Is boutons have P_r 2- to 3-fold higher than those of type Ib boutons (Lu et al., 2016), and a larger proportion of type Ib active zones becomes functional during repeated trains of activity (Newman et al., 2017). We morphologically identified large Ib boutons by size and functionally defined these terminals by eliciting facilitation during a 2 Hz train (Figures 5B and 5E). In contrast, we functionally and anatomically defined small type Is boutons by eliciting the depression characteristic of this motor neuron during a 2 Hz stimulation (Figure 5M). Using these criteria, we observed the expected increase in the amplitude of spontaneous quantal events at both type Ib and type Is terminals of NMJs in vGlut-OE compared with wild-type (Figures 5C and 5K). However, although quantal size was enhanced in vGlut-OE, the total synaptic Ca^{2+} signal following evoked release was significantly reduced compared with wild-type at both type Ib and type Is terminals (Figures 5D, 5E, 5L and 5M), indicating reduced quanta released or bouton (Figures 5G and 5O). This demonstrates that vGlut-OE induces PHD at

both type Ib and type Is motor subtypes, in contrast to *GluRIIA* mutants, in which PHP is exclusively expressed at type Ib synapses (Newman et al., 2017). Therefore, while only PHD signaling and expression occurs at type Is boutons, PHD is induced and expressed at both neuronal subtypes.

Postsynaptic CaMKII Levels Are Unaffected by PHD Signaling

Many lines of evidence suggest that perturbation or loss of GluRIIA-containing postsynaptic GluRs induces PHP expression (Frank et al., 2006; Petersen etal., 1997). Although little is known about the induction mechanism triggering PHP downstream of receptor perturbation, levels of phosphorylated (active) Ca^{2+}/ calmodulin-dependent protein kinase II (pCaMKII) are reduced specifically at postsynaptic densities of type Ib boutons in *GluRIIA* mutants and after PhTx application (Goel et al., 2017; Newman et al., 2017). CaMKII activity is bi-directionally regulated in opposing forms of Hebbian plasticity, long term potentiation (LTP) and long term depression (LTD), in mammalian systems (Coultrap et al., 2014; Pi et al., 2010). We therefore considered that if PHD were a homeostat governing synaptic strength, similar to PHP but in the opposite direction, then postsynaptic pCaMKII levels might be elevated following PHD expression or otherwise altered when PHP and PHD are combined at an individual NMJ. First, we confirmed a ~50% reduction in pCaMKII intensity specifically at type Ib postsynaptic densities of *GluRIIA* mutants (Figures 6A and 6B) and no change in pCaMKII levels in type Is boutons (Figures 6C and 6D). Excess glutamate release and increased mEPSP amplitude could, in principle, enhance pCaMKII levels and induce retrograde PHD signaling in a parallel manner but inverse in direction compared to PHP signaling. However, we observed no significant difference in pCaMKII levels at type Ib or Is postsynaptic densities in vGlut-OE compared to wild-type (Figure 6), revealing that postsynaptic pCaMKII is not modulated during PHD signal transduction. Finally, pCaMKII levels were reduced at type Ib synapses and unchanged at type Is synapses in *GluRIIA* +vGlut-OE (Figure 6), consistent with PHP induction being superimposed on, but not influenced by, PHD expression when both homeo-static processes are triggered at the same NMJ. Thus, a key inductive event involved in PHP signaling in the postsynaptic compartment, pCaMKII, is not regulated during PHD.

PHD Is Not Induced by or Responsive to Increased Postsynaptic Excitability

Various manipulations that disrupt postsynaptic GluRIIA-containing receptors induce retrograde signaling from the muscle to enhance presynaptic glutamate release and stabilize overall synaptic strength (Frank et al., 2006; Petersen et al., 1997). In contrast, the only process known to be capable of inducing PHD at the *Drosophila* NMJ are mutations or manipulations in the presynaptic motor neuron that increase synaptic vesicle size and induce excess vesicular glutamate release (Chen et al., 2014; Daniels et al., 2004; Dickman et al., 2005; Marie et al., 2004; Verstreken et al., 2002). In our final set of experiments, we considered that if PHD was controlled by a homeostat that stabilized overall synaptic strength, similar to PHP but inverse in direction, then a converse perturbation, increased postsynaptic expression of GluRIIA-containing receptors, might induce or modulate PHD expression. However, previous studies demonstrated that when *GluRIIA* is overexpressed, mEPSP amplitude was enhanced, but no compensatory change in presynaptic neurotransmitter release was observed, resulting in increased EPSP amplitude (DiAntonio et

al., 1999; Petersen et al., 1997). We revisited this finding in light of our characterization of PHD by vGlut-OE.

First, we overexpressed the *GluRIIA* subunit in the muscle (GluRIIA-OE), which increased mEPSP amplitudes to levels similar to those of vGlut-OE (Figures 7A and 7B). We confirmed that GluRIIA-OE enhanced GluRIIA-containing receptor abundance without affecting synaptic growth (Figure S4A–4D). However, no change in presynaptic release was observed, leading to a maladaptive, non-homeostatic increase in EPSP amplitude (Figures 7A–7C). Thus, while vGlut-OE and GluRIIA-OE each induce the same enhancement in miniature activity in the postsynaptic cell, only excess presynaptic glutamate release, not increased postsynaptic responsiveness to glutamate, is capable of activating PHD expression. Indeed, we observed no scaling of quantal content as a function of mEPSP amplitude in GluRIIA-OE (Figure S5). Hence, we find no evidence that retrograde communication modulates presynaptic efficacy when muscle excitability is elevated.

We then applied PhTx to GluRIIA-OE synapses, which reduced mEPSP amplitude by ~60% (Figures 7A–7C), as expected. This diminution of mEPSP activity induced an enhancement in presynaptic glutamate release (Figures 7A–7C), demonstrating that PHP can be induced and expressed when elevated postsynaptic GluR levels are acutely perturbed.

Next, we asked whether increasing GluR levels influences PHD expression. We combined both GluRIIA-OE and vGlut-OE manipulations (GluRIIA-OE+vGlut-OE), which led to an enhancement in mEPSP amplitude above either manipulation alone (Figures 7D and 7E). Although EPSP amplitude was also increased in this genotype, quantal content remained the same as vGlut-OE alone (Figures 7D–7F), demonstrating that PHD induction and expression are not influenced by GluRIIA-OE. Finally, application of PhTx to GluRIIA-OE+vGlut-OE NMJs reduced mEPSP amplitude and increased quantal content (Figures 7D–7F).

These results illuminate two important points. First, there is no evidence for the existence of a retrograde homeostatic signaling system that stabilizes synaptic strength when muscle excitability is elevated. Second, PHD operates with complete obliviousness with regard to the state of the postsynaptic cell and to overall synaptic strength, emitting and scaling presynaptic glutamate release independently of the muscle response. This is in contrast to PHP, which is exquisitely sensitive to reduced excitability in the muscle and extremely responsive to reductions in synaptic strength.

Discussion

We have characterized the induction and expression mechanisms driving PHD and PHP alone and defined how synaptic strength is balanced when these two processes are active at the same synapse. While the independent homeostats controlling PHP and PHD result in balanced neurotransmission when induced at the same synapse, this is the result of a superimposition of separate signaling systems operating at disparate and overlapping motor inputs, rather than a deliberate integrated response in the same neuron to stabilize synaptic strength.

Independent Expression Mechanisms Control PHP and PHD

Clearly, distinct genetic mechanisms underlie PHP and PHD signaling, because genes necessary for PHP have no role in PHD. This is illustrated by loss of the gene *dysbindin*, which is required for PHP expression (Dickman and Davis, 2009) but has no impact on PHD, consistent with findings that other genes necessary for PHP do not impact PHD (Gaviño et al., 2015; Kiragasi et al., 2017). Thus, while PHP and PHD appear to be parallel processes that modulate presynaptic neurotransmitter release in inverse directions, they do not employ overlapping genetic machinery.

PHP and PHD also use distinct physiological expression mechanisms. PHD reduces P_r at both type Ib and Is motor neurons (Figure 5) through an apparent reduction in Ca^{2+} influx yet without a change in BRP or the size of the RRP (Gaviño et al., 2015). In contrast, our study and others have found PHP adaptations involve an increase in presynaptic P_r mediated through increased Ca^{2+} influx, active zone scaffolding, Ca^{2+} channel abundance, and enhancement of the RRP (Goel et al., 2017; Gratz et al., 2018; Li et al., 2018; Müller and Davis, 2012; Müller et al., 2012; Weyhersmüller et al., 2011). Indeed, remodeling of BRP at active zones appears to be unique to PHP and to terminals of type Ib boutons. The BRP scaffold controls the size of the RRP (Matkovic et al., 2013) and stabilizes Cac channels at the active zone (Kittel et al., 2006). Therefore, an attractive hypothesis is that PHP requires enhancements in Cac and BRP abundance to promote both Ca^{2+} influx and increase RRP size. Ca^{2+} channels and active zone scaffolds are also homeostatically regulated to control presynaptic neuro-transmitter release in mammalian neurons (Thalhammer et al., 2017), suggesting that such plasticity mechanisms may be evolutionarily conserved.

Distinct Induction Mechanisms Control PHP and PHD Signaling

The postsynaptic induction mechanisms that orchestrate PHP signaling are enigmatic (Chen and Dickman, 2017; Goel et al., 2017). However, it is clear that PHP signaling is extremely sensitive to reductions in postsynaptic excitability, which triggers a compartmentalized intercellular signaling system that originates in the postsynaptic muscle and requires a reduction in CaMKII activity to potentiate neurotransmitter release in the presynaptic neuron (Haghighi et al., 2003; Li et al., 2018; Newman et al., 2017). If PHD were a homeostat designed to stabilize synaptic strength in a way that parallels PHP, then enhanced muscle excitability should induce a retrograde signaling system to depress presynaptic glutamate release. However, our data and previous work demonstrate that homeostatic depression is not induced when quantal size is increased (Petersen et al., 1997). Rather, excess glutamate release from the motor neuron appears to be necessary and sufficient to induce and express PHD. This suggests that an autocrine mechanism triggers PHD signaling, in which excess glutamate is sensed and transduced into a reduction in presynaptic efficacy. Such an autocrine mechanism was astutely proposed as a possibility in the original vGlut-OE study (Daniels et al., 2004).

If an autocrine mechanism mediates PHD induction, this would imply the existence of presynaptic GluRs that can sense excess glutamate and initiate presynaptic inhibition in response. Presynaptic autoreceptors are present and modulate presynaptic function at glutamatergic NMJs of invertebrates and vertebrates (Kiragasi et al., 2017; Pinheiro and

Mulle, 2008). One attractive candidate is the lone metabotropic GluR encoded in the *Drosophila* genome, *mGluRA*. mGluRA is present at presynaptic terminals of motor neurons at the larval NMJ and promotes presynaptic inhibition following excess glutamate released during high-frequency stimulation (Bogdanik et al., 2004). Other possibilities include presynaptic NMDA receptors, which mediate presynaptic inhibition in response to excess glutamate release in the mammalian hippocampus (Padamsey et al., 2017). Notably, NMDA receptors have been reported to be present at the *Drosophila* NMJ (Schuster, 2006). The nature of the glutamate sensor and autocrine signaling system that govern the induction and expression of PHD remains to be defined.

Glutamate Homeostasis at the *Drosophila* NMJ

Why doesn't a homeostat governing synaptic strength exist at the NMJ that is responsive to enhanced postsynaptic excitability? Proper control of muscle contraction is essential to life, and NMJs in many systems use a safety factor that ensures neurotransmitter is released in excess to stably promote muscle contraction. Hence, given this safety factor, it is not clear that a postsynaptic signaling system at the NMJ is necessary to detect and respond to heightened neurotransmitter release or sensitivity. Pharmacological perturbations to cholinergic NMJs that inhibit the enzymatic breakdown of neurotransmitter in worms and mammals lead to rapid paralysis and death, and there is no evidence that homeostatic retrograde signaling systems are initiated to inhibit presynaptic neurotransmitter release during these challenges. Thus, a retrograde homeostatic signaling system to depress presynaptic efficacy in response to increased postsynaptic excitability may not have developed due to a lack of evolutionary pressure.

Why, then, does a process like PHD exist at the *Drosophila* NMJ, designed to inhibit glutamate release through an autocrine presynaptic signaling system? One attractive possibility is that PHD may be a process that maintains stable glutamate levels at the larval NMJ of *Drosophila* in lieu of classical glutamate re-uptake mechanisms. In the CNS, various clearance mechanisms homeostatically maintain ambient glutamate levels to prevent excitotoxicity (Murphy-Royal et al., 2017), and excitatory GluRs are present at presynaptic terminals of the larval *Drosophila* NMJ (Kiragasi et al., 2017). The major mechanism for glutamate clearance in the mammalian brain requires glutamate transporter proteins in the plasma membrane of both glial cells and neurons. In *Drosophila*, there a single excitatory amino acid transporter specific for glutamate reuptake encoded in the genome, *dEAAT1*. *dEAAT1* is expressed in the central nervous system and in peripheral glia at the adult NMJ, where it is involved in glutamate clearance (Rival et al., 2006). However, *dEAAT1* is not expressed at the embryonic or larval NMJ (Rival et al., 2004), and it is unclear how glutamate is controlled in this system. Accordingly, PHD may serve as an adaptive cell autonomous mechanism that responds to excess glutamate and inhibits release to maintain glutamate homeostasis, a process that may have parallels in the mammalian CNS (Padamsey et al., 2017).

Experimental Procedures

Fly Stocks

Drosophila stocks were raised at 25°C on standard molasses food. The w^{1118} strain is used as the wild-type control unless otherwise noted, because this is the genetic background of the transgenic lines and other genotypes used in this study. A complete list of all stocks, genotypes, and details on immunocytochemistry, imaging, and electrophysiology can be found in Supplemental Experimental Procedures.

Immunocytochemistry

Third-instar larvae were dissected in ice cold 0 Ca^{2+} hemolymph-like solution 3 (HL-3) and fixed in either Bouin's fixative or 4% paraformaldehyde (PFA) as described (Perry et al., 2017).

Imaging and Analysis

Samples were imaged using a Nikon A1R resonant scanning confocal microscope as described (Kikuma et al., 2017).

Electrophysiology

All dissections and recordings were performed as described (Kiragasi et al., 2017) in modified HL-3 saline containing 70 mM NaCl, 5 mM KCl, 10 mM $MgCl_2$, 10 mM $NaHCO_3$, 115 mM sucrose, 5 mM trehalose, 5 mM HEPES, and 0.4 mM $CaCl_2$ (unless otherwise specified) (pH 7.2).

Statistical Analysis

All data are presented as mean ± SEM. Data were compared using a one-way ANOVA followed by Tukey's multiple comparison test or using a Student's t test (where specified), analyzed using GraphPad Prism or Microsoft Excel software, with varying levels of significance assessed as *$p < 0.05$, **$p < 0.01$, ***$p < 0.001$, and ****$p < 0.0001$; NS, not significant. A Kruskal-Wallis test in GraphPad Prism was used to assess significance across a set of distributions. See Table S1 for further statistical details and values.

Supplementary Material

Refer to Web version on PubMed Central for supplementary material.

Acknowledgments

We thank Aaron DiAntonio (Washington University, MO, USA) and Graeme Davis (UCSF, CA, USA) for sharing *Drosophila* stocks. We also thank C. Andrew Frank (University of Iowa, IA, USA) and Martin Muller (University of Zurich, Switzerland) for helpful comments and discussions. This work was supported by a grant from the NIH (NS091546) and research fellowships from the Alfred P. Sloan, Ellison Medical, Whitehall, Mallinckrodt, and Klingenstein-Simons Foundations to D.D.

References

Atwood HL, Govind CK, Wu CF. Differential ultrastructure of synaptic terminals on ventral longitudinal abdominal muscles in *Drosophila* larvae. J Neurobiol. 1993; 24:1008–1024. [PubMed: 8409966]

Bogdanik L, Mohrmann R, Ramaekers A, Bockaert J, Grau Y, Broadie K, Parmentier ML. The *Drosophila* metabotropic glutamate receptor DmGluRA regulates activity-dependent synaptic facilitation and fine synaptic morphology. J Neurosci. 2004; 24:9105–9116. [PubMed: 15483129]

Böhme MA, Beis C, Reddy-Alla S, Reynolds E, Mampell MM, Grass-kamp AT, Lützkendorf J, Bergeron DD, Driller JH, Babikir H, et al. Active zone scaffolds differentially accumulate Unc13 isoforms to tune Ca(2+) channel-vesicle coupling. Nat Neurosci. 2016; 19:1311–1320. [PubMed: 27526206]

Chen X, Dickman D. Development of a tissue-specific ribosome profiling approach in *Drosophila* enables genome-wide evaluation of translational adaptations. PLoS Genet. 2017; 13:e1007117. [PubMed: 29194454]

Chen CK, Bregere C, Paluch J, Lu JF, Dickman DK, Chang KT. Activity-dependent facilitation of Synaptojanin and synaptic vesicle recycling by the Minibrain kinase. Nat Commun. 2014; 5:4246. [PubMed: 24977345]

Coultrap SJ, Freund RK, O'Leary H, Sanderson JL, Roche KW, Dell'Acqua ML, Bayer KU. Autonomous CaMKII mediates both LTP and LTD using a mechanism for differential substrate site selection. Cell Rep. 2014; 6:431–437. [PubMed: 24485660]

Cull-Candy SG, Miledi R, Trautmann A, Uchitel OD. On the release of transmitter at normal, myasthenia gravis and myasthenic syndrome affected human end-plates. J Physiol. 1980; 299:621–638. [PubMed: 6103954]

Daniels RW, Collins CA, Gelfand MV, Dant J, Brooks ES, Krantz DE, DiAntonio A. Increased expression of the *Drosophila* vesicular glutamate transporter leads to excess glutamate release and a compensatory decrease in quantal content. J Neurosci. 2004; 24:10466–10474. [PubMed: 15548661]

Davis GW, Müller M. Homeostatic control of presynaptic neuro-transmitter release. Annu Rev Physiol. 2015; 77:251–270. [PubMed: 25386989]

DiAntonio A, Petersen SA, Heckmann M, Goodman CS. Glutamate receptor expression regulates quantal size and quantal content at the *Drosophila* neuromuscular junction. J Neurosci. 1999; 19:3023–3032. [PubMed: 10191319]

Dickman DK, Davis GW. The schizophrenia susceptibility gene *dysbindin* controls synaptic homeostasis. Science. 2009; 326:1127–1130. [PubMed: 19965435]

Dickman DK, Horne JA, Meinertzhagen IA, Schwarz TL. A slowed classical pathway rather than kiss-and-run mediates endocytosis at synapses lacking synaptojanin and endophilin. Cell. 2005; 123:521–533. [PubMed: 16269341]

Frank CA. Homeostatic plasticity at the *Drosophila* neuromuscular junction. Neuropharmacology. 2014; 78:63–74. [PubMed: 23806804]

Frank CA, Kennedy MJ, Goold CP, Marek KW, Davis GW. Mechanisms underlying the rapid induction and sustained expression of synaptic homeostasis. Neuron. 2006; 52:663–677. [PubMed: 17114050]

Gaviño MA, Ford KJ, Archila S, Davis GW. Homeostatic synaptic depression is achieved through a regulated decrease in presynaptic calcium channel abundance. eLife. 2015; 4:e05473.

Goel P, Li X, Dickman D. Disparate Postsynaptic Induction Mechanisms Ultimately Converge to Drive the Retrograde Enhancement of Presynaptic Efficacy. Cell Rep. 2017; 21:2339–2347. [PubMed: 29186673]

Gratz, SJ., Bruckner, JJ., Hernandez, RX., Khateeb, K., Macleod, G., O'Connor-Giles, KM. Calcium channel levels at single synapses predict release probability and are upregulated in homeostatic potentiation. bioRxiv. 2018. https://doi.org/10.1101/240051

Haghighi AP, McCabe BD, Fetter RD, Palmer JE, Hom S, Goodman CS. Retrograde control of synaptic transmission by post-synaptic CaMKII at the Drosophila neuromuscular junction. Neuron. 2003; 39:255–267. [PubMed: 12873383]

Kidokoro Y, Kuromi H, Delgado R, Maureira C, Oliva C, Labarca P. Synaptic vesicle pools and plasticity of synaptic transmission at the *Drosophila* synapse. Brain Res Brain Res Rev. 2004; 47:18–32. [PubMed: 15572160]

Kikuma K, Li X, Kim D, Sutter D, Dickman DK. Extended Synaptotagmin Localizes to Presynaptic ER and Promotes Neurotransmission and Synaptic Growth in *Drosophila*. Genetics. 2017; 207:993–1006. [PubMed: 28882990]

Kiragasi B, Wondolowski J, Li Y, Dickman DK. A Presynaptic Glutamate Receptor Subunit Confers Robustness to Neurotransmission and Homeostatic Potentiation. Cell Rep. 2017; 19:2694–2706. [PubMed: 28658618]

Kittel RJ, Wichmann C, Rasse TM, Fouquet W, Schmidt M, Schmid A, Wagh DA, Pawlu C, Kellner RR, Willig KI, et al. Bruchpilot promotes active zone assembly, Ca2+ channel clustering, and vesicle release. Science. 2006; 312:1051–1054. [PubMed: 16614170]

Li X, Goel P, Chen C, Angajala V, Chen X, Dickman D. Synapse-specific and compartmentalized expression of presynaptic homeostatic potentiation. eLife. 2018; 7:e34338. [PubMed: 29620520]

Lu Z, Chouhan AK, Borycz JA, Lu Z, Rossano AJ, Brain KL, Zhou Y, Meinertzhagen IA, Macleod GT. High-Probability Neurotransmitter Release Sites Represent an Energy-Efficient Design. Curr Biol. 2016; 26:2562–2571. [PubMed: 27593375]

Marie B, Sweeney ST, Poskanzer KE, Roos J, Kelly RB, Davis GW. Dap160/intersectin scaffolds the periactive zone to achieve high-fidelity endocytosis and normal synaptic growth. Neuron. 2004; 43:207–219. [PubMed: 15260957]

Matkovic T, Siebert M, Knoche E, Depner H, Mertel S, Owald D, Schmidt M, Thomas U, Sickmann A, Kamin D, et al. The Bruchpilot cytomatrix determines the size of the readily releasable pool of synaptic vesicles. J Cell Biol. 2013; 202:667–683. [PubMed: 23960145]

Müller M, Davis GW. Transsynaptic control of presynaptic Ca^{2+} influx achieves homeostatic potentiation of neurotransmitter release. Curr Biol. 2012; 22:1102–1108. [PubMed: 22633807]

Müller M, Liu KS, Sigrist SJ, Davis GW. RIM controls homeo-static plasticity through modulation of the readily-releasable vesicle pool. J Neurosci. 2012; 32:16574–16585. [PubMed: 23175813]

Murphy-Royal C, Dupuis J, Groc L, Oliet SHR. Astroglial glutamate transporters in the brain: Regulating neurotransmitter homeostasis and synaptic transmission. J Neurosci Res. 2017; 95:2140–2151. [PubMed: 28150867]

Newman ZL, Hoagland A, Aghi K, Worden K, Levy SL, Son JH, Lee LP, Isacoff EY. Input-Specific Plasticity and Homeostasis at the Drosophila Larval Neuromuscular Junction. Neuron. 2017; 93:1388–1404e10. [PubMed: 28285823]

Padamsey Z, Tong R, Emptage N. Glutamate is required for depression but not potentiation of long-term presynaptic function. eLife. 2017; 6:e29688. [PubMed: 29140248]

Perry S, Han Y, Das A, Dickman D. Homeostatic plasticity can be induced and expressed to restore synaptic strength at neuromuscular junctions undergoing ALS-related degeneration. Hum Mol Genet. 2017; 26:4153–4167. [PubMed: 28973139]

Petersen SA, Fetter RD, Noordermeer JN, Goodman CS, DiAntonio A. Genetic analysis of glutamate receptors in *Drosophila* reveals a retrograde signal regulating presynaptic transmitter release. Neuron. 1997; 19:1237–1248. [PubMed: 9427247]

Pi HJ, Otmakhov N, Lemelin D, De Koninck P, Lisman J. Autonomous CaMKII can promote either long-term potentiation or long-term depression, depending on the state of T305/T306 phosphorylation. J Neurosci. 2010; 30:8704–8709. [PubMed: 20592192]

Pozo K, Goda Y. Unraveling mechanisms of homeostatic synaptic plasticity. Neuron. 2010; 66:337–351. [PubMed: 20471348]

Pinheiro PS, Mulle C. Presynaptic glutamate receptors: physiological functions and mechanisms of action. Nat Rev Neurosci. 2008; 9:423–436. [PubMed: 18464791]

Rival T, Soustelle L, Strambi C, Besson MT, Iché M, Birman S. Decreasing glutamate buffering capacity triggers oxidative stress and neuropil degeneration in the *Drosophila* brain. Curr Biol. 2004; 14:599–605. [PubMed: 15062101]

Rival T, Soustelle L, Cattaert D, Strambi C, Iché M, Birman S. Physiological requirement for the glutamate transporter dEAAT1 at the adult *Drosophila* neuromuscular junction. J Neurobiol. 2006; 66:1061–1074. [PubMed: 16838372]

Schuster CM. Experience-dependent potentiation of larval neuro-muscular synapses. Int Rev Neurobiol. 2006; 75:307–322. [PubMed: 17137934]

Thalhammer A, Contestabile A, Ermolyuk YS, Ng T, Volynski KE, Soong TW, Goda Y, Cingolani LA. Alternative Splicing of P/Q-Type Ca^{2+} Channels Shapes Presynaptic Plasticity. Cell Rep. 2017; 20:333–343. [PubMed: 28700936]

Turrigiano G. Homeostatic synaptic plasticity: local and global mechanisms for stabilizing neuronal function. Cold Spring Harb Perspect Biol. 2012; 4:a005736. [PubMed: 22086977]

Turrigiano GG. The dialectic of Hebb and homeostasis. Philos Trans R Soc Lond B Biol Sci. 2017; 372:20160258. [PubMed: 28093556]

Verstreken P, Kjaerulff O, Lloyd TE, Atkinson R, Zhou Y, Meinertzhagen IA, Bellen HJ. Endophilin mutations block clathrin-mediated endocytosis but not neurotransmitter release. Cell. 2002; 109:101–112. [PubMed: 11955450]

Weyhersmüller A, Hallermann S, Wagner N, Eilers J. Rapid active zone remodeling during synaptic plasticity. J Neurosci. 2011; 31:6041–6052. [PubMed: 21508229]

Highlights

- Two independent homeostats bi-directionally control presynaptic efficacy in Drosophila
- Homeostatic potentiation and depression are expressed at distinct neuronal subtypes
- Homeostatic depression is not induced or influenced through postsynaptic excitability
- An autocrine signaling mechanism responds to excess glutamate to induce depression

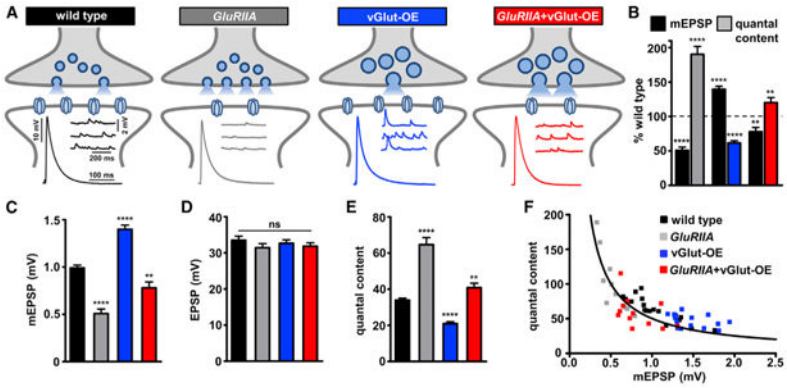

Figure 1. Presynaptic Homeostatic Potentiation and Depression Can Be Induced, Expressed, and Balanced

(A) Schematic of genetic manipulations to the *Drosophila* NMJ that induce bi-directional, homeostatic changes in presynaptic neurotransmitter release over chronic timescales. Presynaptic homeostatic potentiation (PHP) is observed when mEPSP amplitudes are reduced due to genetic loss of the postsynaptic GluR subunit *GluRIIA*. Presynaptic homeostatic synaptic depression (PHD) is observed when mEPSP amplitudes are enhanced following overexpression of the vesicular glutamate transporter in motor neurons (vGlut-OE). Synaptic strength (EPSP amplitude) is maintained at baseline levels when PHP and PHD are individually expressed or combined at an individual NMJ in *GluRIIA*+vGlut-OE. Insets: representative electrophysiological traces in the indicated genotypes, each showing similar EPSP amplitudes despite differences in mEPSP amplitudes.

(B) Quantification of mEPSP amplitude and quantal content in the indicated genotypes (coded by color), normalized to wild-type values. A homeostatic increase in presynaptic glutamate release (quantal content) is observed in *GluRIIA* mutants, while a homeostatic decrease is observed in vGlut-OE. When combined, *GluRIIA*+vGlut-OE show similar mEPSP and quantal content values compared to wild-type.

(C–E) Quantification of mEPSP amplitude (C), EPSP amplitude (D), and quantal content (E) in the indicated genotypes.

(F) All genotypes show homeostatic tuning of quantal content over varying average quantal sizes, in effect maintaining stable levels of synaptic strength. The black curve represents ideal homeostatic tuning, derived by solving the function of EPSP = QC × mEPSP. QC, quantal content.

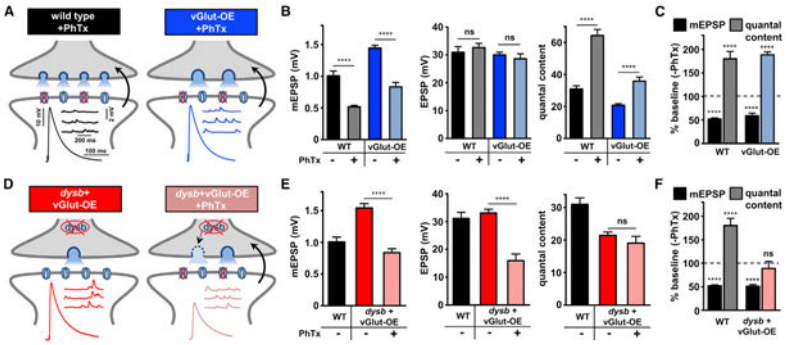

Figure 2. Conventional Mechanisms Are Required for the Acute Expression of PHP in vGlut-OE

(A) Schematic and representative traces of wild-type and vGlut-OE NMJs following the acute application of PhTx. Diminished mEPSP amplitudes are observed in both wild-type and vGlut-OE NMJs after PhTx application, while EPSP amplitudes are maintained at baseline levels due to a homeostatic increase in quantal content.

(B) Quantification of mEPSP amplitude, EPSP amplitude, and quantal content values in the indicated genotypes and conditions.

(C) mEPSP and quantal content values following PhTx application normalized as a percentage of baseline values (no PhTx treatment).

(D) Schematic and representative traces of vGlut-OE in a *dysbindin* mutant background (*dysb*+vGlut-OE) in baseline conditions and following application of PhTx. While loss of *dysbindin* has no impact on PHD expression, PHP expression is blocked following application of PhTx to *dysb*+vGlut-OE.

(E) Quantification of mEPSP amplitude, EPSP amplitude, and quantal content values in the indicated genotypes and conditions.

(F) Quantification of mEPSP and quantal content values normalized to baseline values.

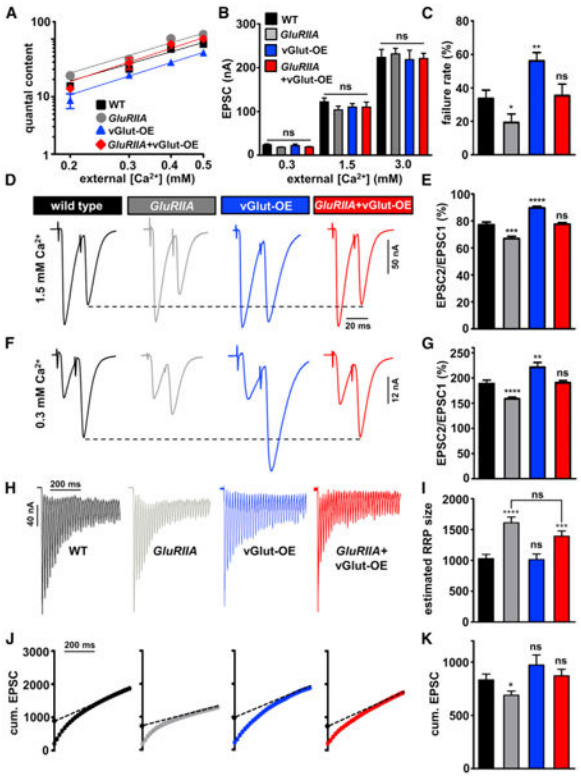

Figure 3. Characterization of Ca^{2+} Co-operativity, Failure Analysis, and RRPs in *GluRIIA* +vGlut-OE

(A) Quantal content plotted as a function of extracellular Ca^{2+} concentration on a log/log scale, with best fit lines shown, for the indicated genotypes. No significant differences in the slopes were observed (Table S1).

(B) EPSC amplitude following homeostatic challenge remains similar to wild-type in the indicated genotypes across a range of extracellular Ca^{2+} conditions.

(C) Failure analysis reveals a decrease in failure rate in *GluRIIA* mutants, while an increase in failure rate is observed in vGlut-OE, as expected. An intermediate failure rate is observed in *GluRIIA*+vGlut-OE, consistent with a balancing of adaptations resulting from both PHP and PHD expression. Recordings were performed in 0.05 mM extracellular Ca^{2+}.

(D) Representative paired-pulse EPSC traces at 1.5 mM extracellular Ca^{2+} with an interstimulus interval of 16.7 ms in the indicated genotypes. Enhanced paired-pulse depression (PPD) was observed in *GluRIIA* mutants, while reduced PPD was found in vGlut-OE, consistent with increased and reduced probability of release.

(E) Quantification of the paired-pulse ratio (EPSC2/EPSC1) in the indicated genotypes.

(F) Representative paired-pulse EPSC traces at 0.3 mM extracellular Ca^{2+} in the indicated genotypes. Reduced paired-pulse facilitation (PPF) was observed in *GluRIIA* mutants, while enhanced PPF was found in vGlut-OE, consistent with increased and reduced probability of release.

(G) Quantification of the paired-pulse ratio (EPSC2/EPSC1) in the indicated genotypes.

(H) Representative EPSC recordings of 30 stimuli at 3 mM extracellular Ca^{2+} during a 60 Hz stimulus train in the indicated genotypes.

(I) Estimated size of the RRP in the indicated genotypes demonstrating the RRP is increased in both *GluRIIA* mutants and *GluRIIA*+vGlut-OE.
(J) Average cumulative EPSC amplitude plotted as a function of time. A line fit to the 18th–30th stimuli was back-extrapolated to time 0.
(K) Average cumulative EPSC values for the indicated genotypes.

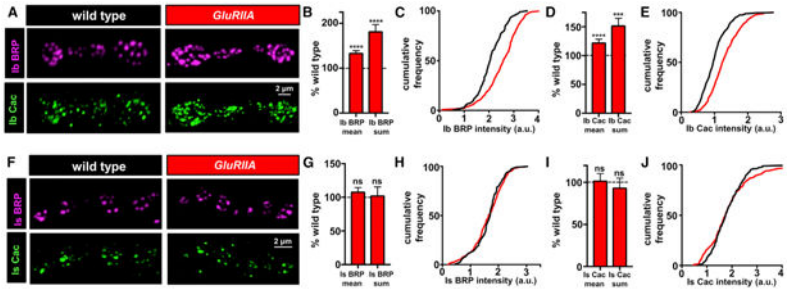

Figure 4. BRP and Cac Abundance in Active Zones Are Specifically Enhanced at Type Ib Terminals in *GluRIIA* Mutants

(A) Representative images of type Ib boutons immunostained with anti-GFP and anti-BRP at NMJs transgenically overexpressing the Ca^{2+} channel Cac-GFP in the indicated genotypes.

(B–E) Quantification of mean and sum immunofluorescence intensity of BRP (B) and Cac-GFP-OE (D) puncta and cumulative frequency distribution of mean BRP (C) and Cac-GFP-OE (E) puncta at type Ib boutons reveal a significant increase in these values in *GluRIIA* mutants.

(F) Representative images of type Is boutons with the same immunolabeling and genotypes as in (A).

(G–J) No changes in BRP or Cac-GFP mean or sum puncta intensity (G and I) or cumulative frequency distribution (H and J) are observed at type Is boutons in *GluRIIA* mutants.

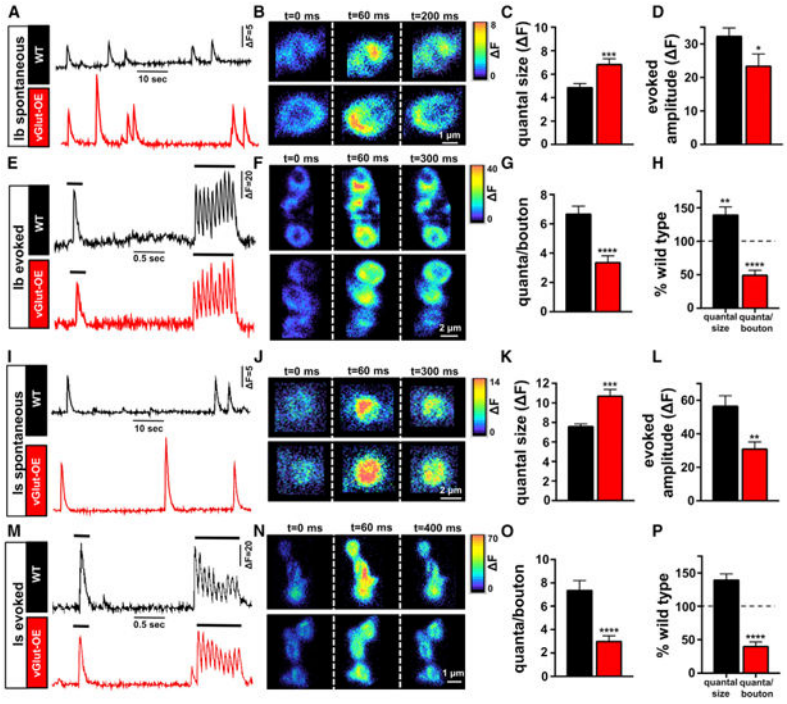

Figure 5. *In Vivo* Ca^{2+} Imaging Reveals Both Type Ib and Type Is Boutons Express PHD

(A) Representative traces of spontaneous Ca^{2+} transients imaged at type Ib boutons in the indicated genotypes. Consistent with electrophysiological recordings, vGlut-OE synapses show enhanced miniature Ca^{2+} signals compared to wild-type (WT).

(B) Representative images of spontaneous GCaMP signals coded as a heatmap at individual type Ib boutons shown at three time points. The change in fluorescence (ΔF) during a spontaneous event is larger at vGlut-OE type Ib boutons.

(C and D) Quantification of quantal size (ΔF of the spontaneous Ca^{2+} transient event) (C) and evoked Ca^{2+} transient event (D) at individual boutons.

(E) ΔF traces of a single evoked event followed by a 2 Hz stimulus train to functionally define type Ib boutons based on their characteristic facilitation. Note the reduced evoked response at type Ib boutons in vGlut-OE.

(F) Representative images of evoked GCaMP signals.

(G) Reduced quanta released per bouton per evoked stimulus at vGlut-OE NMJs compared to wild-type, indicative of PHD expression.

(H) Quantal size and quanta released per bouton in vGlut-OE normalized to wild type.

(I) Ca^{2+} transients during spontaneous events at type Is boutons. vGlut-OE boutons show enhanced Ca^{2+} signals compared to WT.

(J) Representative images of spontaneous GCaMP signals at individual type Is boutons.

(K and L) Quantal size is enhanced at type Is boutons in vGlut-OE (K), and the evoked Ca^{2+} transient event per individual bouton is significantly reduced (L).

(M) ΔF traces of an individual bouton stimulus followed by a 2 Hz train functionally defines type Is boutons by their characteristic depression.

(N) Representative images of evoked GCaMP signals at type Is boutons shown at three time points.

(O) Reduced quanta is released per bouton in vGlut-OE, indicative of PHD expression.
(P) Quantal size and quanta released per bouton in vGlut-OE normalized to wild type.

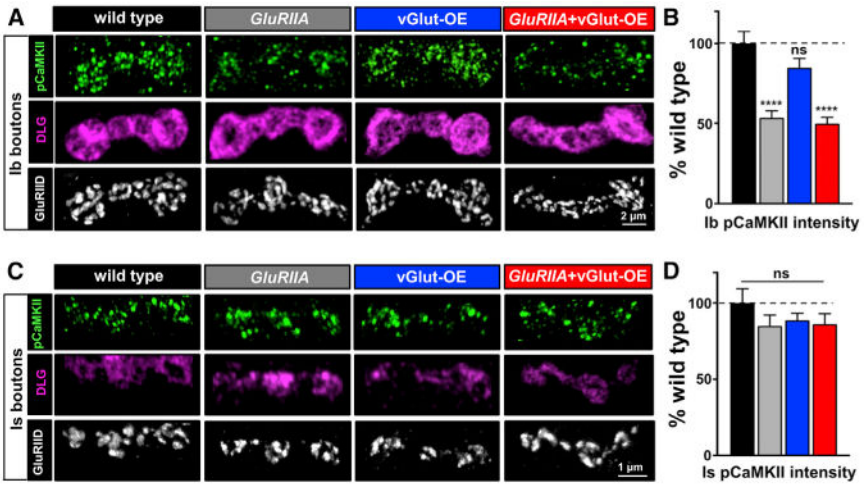

Figure 6. pCaMKII Levels Are Reduced Specifically at Type Ib Postsynaptic Densities in *GluRIIA* Mutants and Unchanged in vGlut-OE

(A) Representative images of NMJs immuno-stained with antibodies that recognize the active (phosphorylated) form of CaMKII (pCaMKII), the postsynaptic scaffold discs large (DLG), and the essential postsynaptic GluR subunit GluRIID.

(B) Quantification of total pCaMKII intensity at muscle 6/7 type Ib boutons reveals a reduction in *GluRIIA* and *GluRIIA*+vGlut-OE and no significant change in vGlut-OE.

(C) Representative images of type Is boutons immunostained in the same conditions and genotypes as in (A).

(D) Quantification of pCaMKII intensity at type Is boutons shows no significant change in any genotype, consistent with PHP not operating at type Is boutons and PHD having no impact on post-synaptic pCaMKII levels.

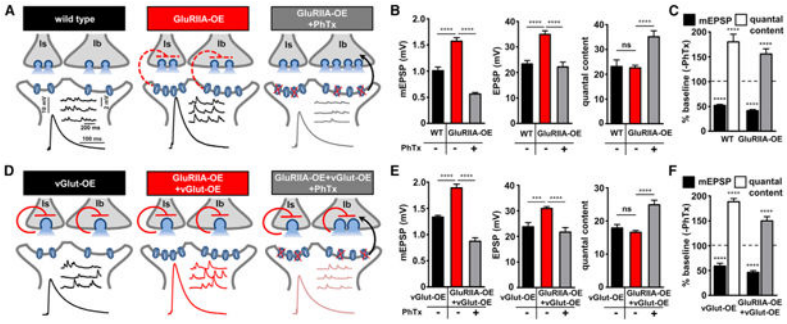

Figure 7. Enhanced Quantal Size Triggered by Postsynaptic Overexpression of *GluRIIA* Does Not Induce or Modulate PHD Expression

(A) Schematic and representative traces of postsynaptic overexpression of the *GluRIIA* subunit (GluRIIA-OE) at baseline conditions and after PhTx application. Although GluRIIA-OE increases mEPSP amplitude, no change in presynaptic neurotransmitter release is observed, leading to enhanced EPSP amplitude and no change in quantal content. Hence, enhanced mEPSP amplitude through postsynaptic mechanisms does not induce retrograde PHD signaling (schematized by the red dashed arrow). After PhTx application to GluRIIA-OE, mEPSP amplitude is reduced, while retrograde PHP signaling is induced, leading to a homeostatic increase in quantal content.

(B) Quantification of average mEPSP amplitude, EPSP amplitude, and quantal content values for the indicated genotypes and conditions.

(C) mEPSP and quantal content values normalized to baseline conditions (−PhTx).

(D) Schematic and representative traces of vGlut-OE combined with GluRIIA-OE alone and after PhTx application. In this condition, GluRIIA-OE+vGlut-OE, mEPSP amplitudes are further enlarged, but PHD is normally expressed, resulting in no change in quantal content compared with vGlut-OE alone. An autocrine mechanism requiring excess glutamate release to induce PHD is schematized by the red arrow. Acute PhTx application induces PHP expression in GluRIIA-OE+vGlut-OE.

(E) Quantification of mEPSP amplitude, EPSP amplitude, and quantal content values in the indicated genotypes and conditions.

(F) Quantification of mEPSP and quantal content values normalized to baseline values (−PhTx).